

Quantitative analysis of morphometric parameters of fascicular groups of peripheral nerve on MicroCT images

Yingchun ZHONG¹, Jian QI², Peng LUO³, Fang LI⁴, Shuang ZHU⁵

1 School of Automation, Guangdong University of Technology, Guangzhou 510006, China.

2 Department of Microsurgery-Orthopedic Trauma & Hand-surgery, The First Affiliated Hospital of Sun Yat-sen University, Guangzhou 510080, China.

3 Department of Orthopedics, the Sixth People's Hospital of Shenzhen, Shenzhen 518060, China.

4 School of Information, Guangdong University of Finance and Economics, Guangzhou 510300, China

5 Department of Orthopedics, the Second Affiliated Hospital of Southern Medical University, Guangzhou 510300, China.

Correspondence to: Peng Luo
 No. 89 Taoyuan Road, Nanshan District, Shenzhen City, Guangdong,
 518060, China
 E-MAIL: luopeng729@yandex.com

Submitted: 2020-11-23 *Accepted:* 2021-02-05 *Published online:* 2021-02-05

Key words: **Peripheral nerve; MicroCT; Fascicular group; Morphological parameter; Quantification**

Neuroendocrinol Lett 2021; **42**(2):70–80 PMID: 34217163 NEL420121A05 © 2021 Neuroendocrinology Letters • www.nel.edu

Abstract

BACKGROUND: Sectional image of the peripheral nerves is a prerequisite for studying the morphological parameters of fascicular groups. Ultra-high precision MicroCT scan can explicitly display the internal morphology of physiological tissues. This study aimed to quantitatively measure the basic morphological parameters of fascicular groups of a peripheral nerve on MicroCT images, obtain the statistical principles and investigate the variation pattern of these morphological parameters during the process of fascicular group extension.

METHODS: Peripheral nerve specimens were processed with fat removal, decellularization, freezing, and drying, *etc.* The morphological parameters including area, perimeter, and the degree of circularity of each fascicular group in the peripheral nerve on MicroCT images were obtained by the image processing method. The cross-sectional area, cross-sectional perimeter, and cross-sectional degree of circularity of the single fascicular group were analyzed. Correlation between the cross-sectional area of single fascicular group and fascicular group extension, the correlation between the perimeter of cross-sectional single fascicular group and fascicular group extension, and correlation between the cross-sectional degree of circularity of single fascicular group and fascicular group extension were analyzed.

RESULTS: The cross-sectional area of fascicular groups confirmed the *Beta* distribution with a dominant proportion of small-area fascicular groups and a low percentage of large-area fascicular groups. Within the range of 3 mm, no significant correlation was observed between the cross-sectional area and the spatial extension of fascicular groups. The perimeter of the fascicular group section was normally distributed. The perimeter of the fascicular group section that did not remain stable immediately after the fascicular group - was split or merged, but it gradually became stable after the fascicular groups extended to a certain distance.

The cross-sectional area of the fascicular groups did not change significantly during this period. The degree of circularity of the fascicular group section followed the t distribution pattern with scale/position parameters. Similarly, it gradually approached the average value only after the fascicular groups extended to a certain length.

CONCLUSION: Current study revealed the general rules of the basic morphometric parameters of fascicular groups in the process of spatial extension, which provided a pivotal basis for the repair of peripheral nerves and the diagnosis and treatment of neurological diseases and was of academic value and significance.

INTRODUCTION

The peripheral nerve of the limbs is the main channel that connects the trunk and limbs, which plays a role in transmitting sensory impulses and issuing motion instructions (Zhang et al. 2009). The basic morphological parameters of the fascicular group inside the peripheral nerve mainly include the area, perimeter, and degree of circularity of the fascicular groups. Investigating the morphological parameters of these fascicular groups and the variation principle following the spatial extension of the fascicular groups can provide references for peripheral nerve repair and diagnosis and treatment of relevant diseases (Raj et al. 2017; Li et al. 2012; Al-Fahdawi et al. 2016).

Li et al. have employed molecular hyperspectral imaging technology to process the spinal nerve fiber, obtain microscopic images of nerve fibers, and extract morphological parameters, such as myelin thickness and area (Li et al. 2012). Eye tracking-assisted spectrum-domain optical coherence tomography has been adopted to extract the thickness of the retinal nerve fiber layer (RNFL) (Rajjoub et al. 2015). Páll Karlsson et al. have proposed that quantitative evaluation of morphological parameters, such as intraepidermal nerve fiber density, contributed to the diagnosis of differential symmetric polyneuropathy (Karlsson et al. 2016). Anisotropic diffusion filtering combined with morphological processing is deployed to segment the optic nerve on microscopic images, and evaluate the changes of morphometric parameters of the optic nerve (Al-Fahdawi et al. 2016). Also, MR scan has been utilized to measure the morphological and relaxometric changes of the distal tibial nerves under chronic inflammatory demyelinating polyneuropathy (Felisaz et al. 2019), suggesting that the study of morphometric parameters of nerves and fascicular groups can provide a valuable basis for the diagnosis and treatment of neurological diseases.

Sectional image of fascicular groups of the peripheral nerves is a prerequisite for investigating the morphological parameters of fascicular groups. At present, two methods are primarily available to obtain the sectional images of fascicular groups: slice preparation

and MicroCT scanning methods. The slice photographing method requires slicing, dyeing, scanning, photographing, splicing and registration, etc., which is inefficient and yields low precision (Zhong et al. 2015; Zhong et al. 2011; Zhong et al. 2012). Ultra-high precision MicroCT scan can explicitly display the internal morphology of physiological tissues, which has been employed to scan the nerve and blood vessels to construct the spatial structures (Hipp et al. 2009). Watling et al. have adopted metal osmium compounds to dye the sciatic nerve of mice, and then fix the sciatic nerve on a polymer scaffold and subject to low-dose X-ray irradiation on a MicroCT device to evaluate the blood supply of nerve blood vessels to the nerve and the regeneration of fascicular group (Watling et al. 2010). Besides, a MicroCT scan has been utilized to scan the rat sciatic nerve to observe the regeneration of fascicular groups (Hopkins et al. 2015). Zhu and Yan from Sun Yat-sen University have used MicroCT to scan peripheral nerves and construct a three-dimensional structure including fascicular groups and connective tissues (Zhu et al. 2016; Yan et al. 2017). All these studies explored the application of ultra-high precision MicroCT scan in anatomical structures of peripheral nerve, laid a consolidated foundation for analyzing the morphometric parameters of fascicular groups of the peripheral nerves.

In this study, morphometric parameters, such as area, perimeter, and circularity of each fascicular group in each peripheral nerve on MicroCT image were obtained through image processing and calculation. Subsequently, the maximum, average, and minimum values of these morphometric parameters in the process of spatial extension are calculated and recorded to analyze the probability distribution pattern of these morphological parameters. In addition, the correlation between these morphometric parameters and the spatial extension of the fascicular group was evaluated.

MATERIALS AND METHODS

Sampling collection

Peripheral nerve specimens were processed with fat removal, decellularization, freezing, and drying, etc. To adapt to the parameter constrictions of MicroCT equipment, the long-segment peripheral nerve was cut into small segments with a length of approximately 4 mm for a subsequent experiment (Figure 1A). A total of 8 specimens were eventually obtained, as illustrated in Figure 1B. The redundant part of the nerve was preserved for a subsequent experiment. This study was approved by the Institutional Review Board of Shenzhen Nanshan people's hospital (No. [2019]072645).

MicroCT scan

The MicroCT scanning of specimens was illustrated in Figure 1C. The default parameters of the MicroCT scan were selected as previously described (Zhu et al. 2016).

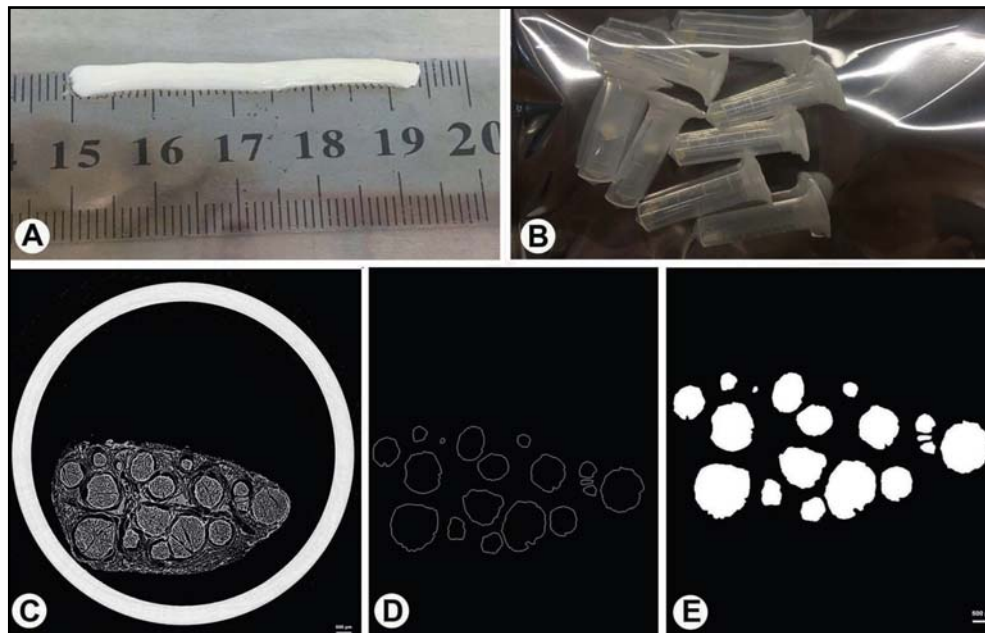


Fig. 1. Peripheral nerve specimen processing and collection. A. Peripheral nerve length measurement; B. Specimen collected in tube after cutting into small pieces; C. MicroCT scan results (the 10th image of the 2nd specimen); D. Contour of the fascicular groups on the 10th image; E. fascicular groups displayed in high-brightness pixels.

According to the MicroCT scanning images, the 10th image of the 2nd specimen was chosen to acquire the contour of fascicular groups, as shown in Figure 1D by using the methods as previously described in research (Zhong *et al.* 2015). The contour and area of a fascicular group which was expressed by high-brightness pixels were selected, as described in Figure 1E.

Quantitative analysis of a cross-sectional area of single fascicular group

The cross-sectional area of a single fascicular group on the MicroCT scan image is defined as the number of pixels surrounded by the inner region of the fascicular group as below.

$$s_{i,j} = \text{Inner_Num}_{i,j} \quad (1)$$

In which, $\text{Inner_Num}_{i,j}$ refers to the number of high-brightness pixels of the i fascicular group on the j MicroCT scan image.

All specimens were scanned with the same MicroCT scanning parameters, and then the cross-sectional area of each fascicular group on all MicroCT images was calculated. The maximum, minimum, and average area could be obtained to acquire the corresponding statistical distribution pattern.

Correlation analysis between cross-sectional area of single fascicular group and fascicular group extension

During the MicroCT scan, the serial scanning images of the fascicular group section could be acquired. In other words, the number of the scanning image

represented a specific position of the fascicular group in the spatial extension process. Therefore, the correlation between the cross-sectional area of the fascicular group and the fascicular group extension referred to the correlation between the cross-sectional area of the fascicular group and the serial numbering of MicroCT scanning image:

$$s_{i,j} = f(j) \quad j = 1, 2, \dots, m \quad (3)$$

m is the total number of images scanned for a specimen. $s_{i,j}$ is the area of the i root fascicular group on the j scan image.

Quantitative analysis of cross-sectional perimeter of the single fascicular group

The cross-sectional perimeter of a single fascicular group on the MicroCT image is defined as the number of pixels of the cross-sectional border of the fascicular group.

$$p_{i,j} = \text{Border_Num}_{i,j} \quad (4)$$

$\text{Border_Num}_{i,j}$ is the number of pixels of the border of the i fascicular group on the j MicroCT image.

Correlation analysis between the perimeter of cross-sectional single fascicular group and fascicular group extension

The correlation between the perimeter of the cross-sectional single fascicular group and the fascicular group extension can be established by analyzing the

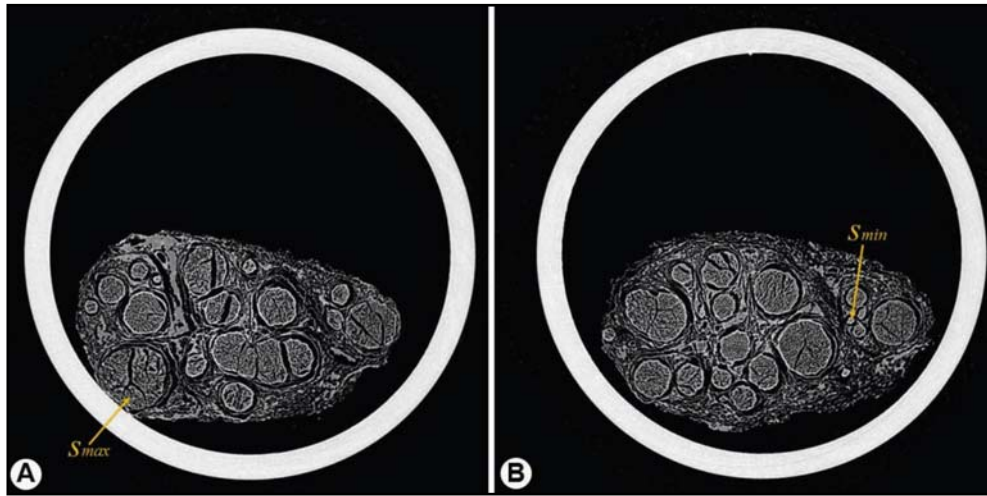


Fig. 2. Single fascicular group with the maximal area on the 139th image (A); single fascicular group with the minimal area on the 440th image (B).

correlation between the circumference of the cross-sectional perimeter of the fascicular group and the number of scanning images.

$$p_{i,j} = f(j) \quad j = 1, 2 \dots m \quad (5)$$

m is the total number of scanning images of a certain specimen.

Quantitative analysis of cross-sectional degree of circularity of single fascicular group

The degree of circularity of the cross-sectional fascicular group is defined as:

$$c_{i,j} = \frac{4\pi \cdot s_{i,j}}{p_{i,j}^2} \quad (6)$$

$c_{i,j}$ refers to the degree of circularity of the i fascicular group on the j MicroCT image.

Correlation analysis between cross-sectional degree of circularity of single fascicular group and fascicular group extension

The correlation between the cross-sectional degree of circularity of a single fascicular group and fascicular group extension can be established by analyzing the correlation between the cross-sectional degree of circularity of the fascicular group and the number of scanning images.

$$c_{i,j} = f(j) \quad j = 1, 2 \dots m \quad (7)$$

m is the total number of scanning images of a certain specimen.

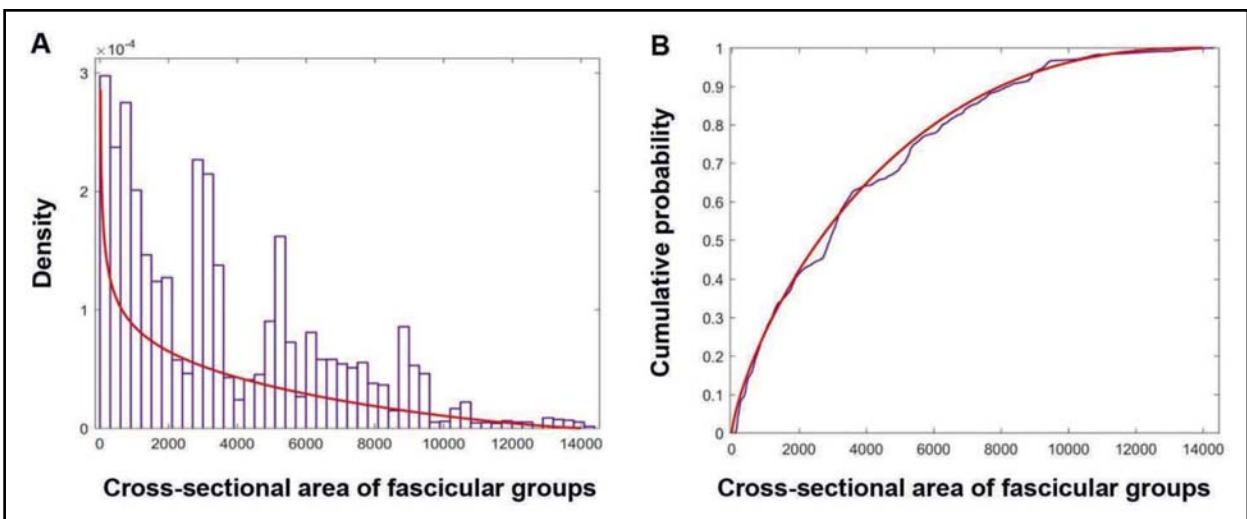


Fig. 3. Probability distribution of fascicular group area; histogram and probability density of area (A), cumulative probability of area (B).

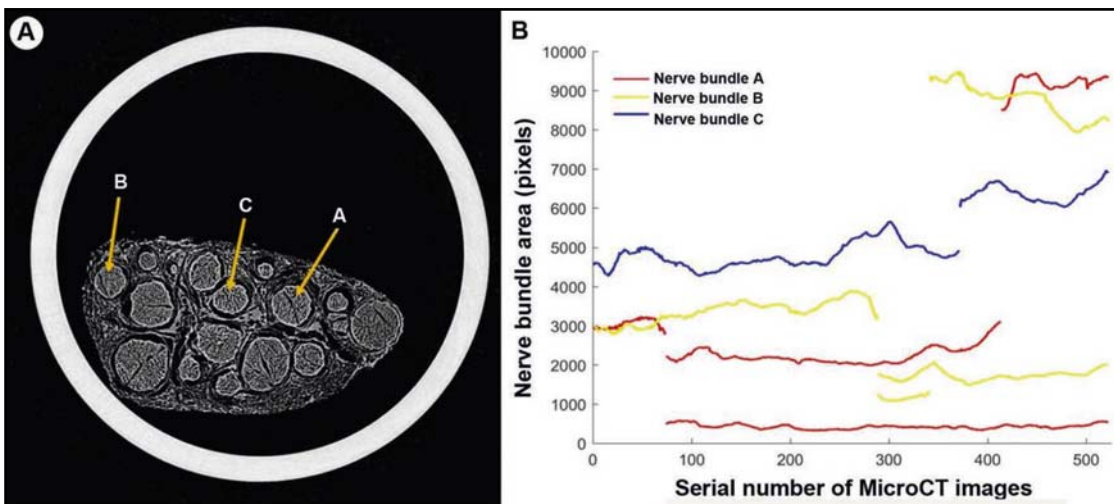


Fig. 4. MicroCT images of fascicular groups A, B and C (A); the curve of area changes of fascicular groups A, B and C over spatial extension.

RESULTS

Cross-sectional area of single fascicular group

MicroCT imaging was adopted to scan all specimens and 4,621 images were obtained. Then, all scanning images were processed by image processing software to obtain Figure 1D. Morphological parameters, such as area and perimeter of the highlighted areas on these images were obtained. The maximum cross-sectional area of single fascicular group: $s_{max} = 14322pixels$, where it appears as illustrated in the fascicular group in Figure 2A. The fascicular group was located on the 139th scanning image of the specimen.

The minimal cross-sectional area of the single fascicular group on the 440th scanning image of this specimen: $s_{min} = 87pixels$, as illustrated in Figure 2B.

The mean cross-sectional area of the single fascicular group: $s_{mean} = 3563.4pixels$.

The histogram of the cross-sectional area of the fascicular group is illustrated in Figure 3A. According to the probability distribution fitting of the histogram, it can be observed that the cross-sectional area of the fascicular group followed the *Beta* distribution pattern. The probability density function curve is shown in the red curve in Figure 3A, and its probability density function is:

$$f(x|\alpha, \beta) = 87 + \frac{14200}{B(\alpha, \beta)} \cdot x^{\alpha-1} \cdot (1-x)^{\beta-1} \quad (2)$$

In which $B(\alpha, \beta) = \frac{\Gamma(\alpha) \cdot \Gamma(\beta)}{\Gamma(\alpha + \beta)}$, $\alpha = 0.741$, $\beta = 2.29$, $\Gamma(*)$ is gamma function.

The cumulative probability distribution diagram of the fascicular group cross-sectional area is shown in Figure 3B. The blue curve refers to the actual cumulative

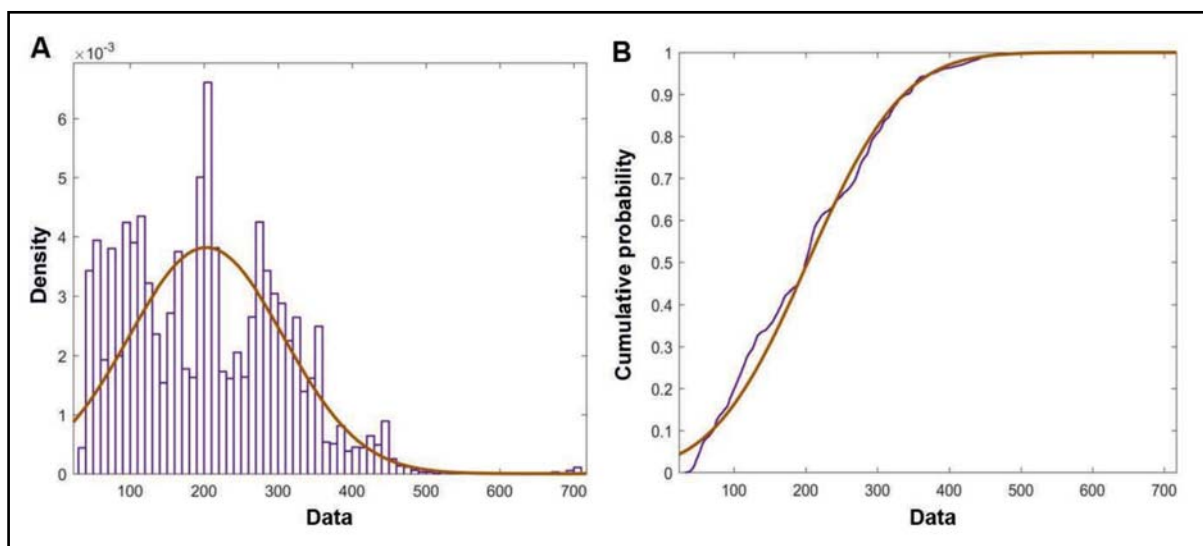


Fig. 5. Histogram of probability density (A) and cumulative probability of fascicular group perimeter (B).

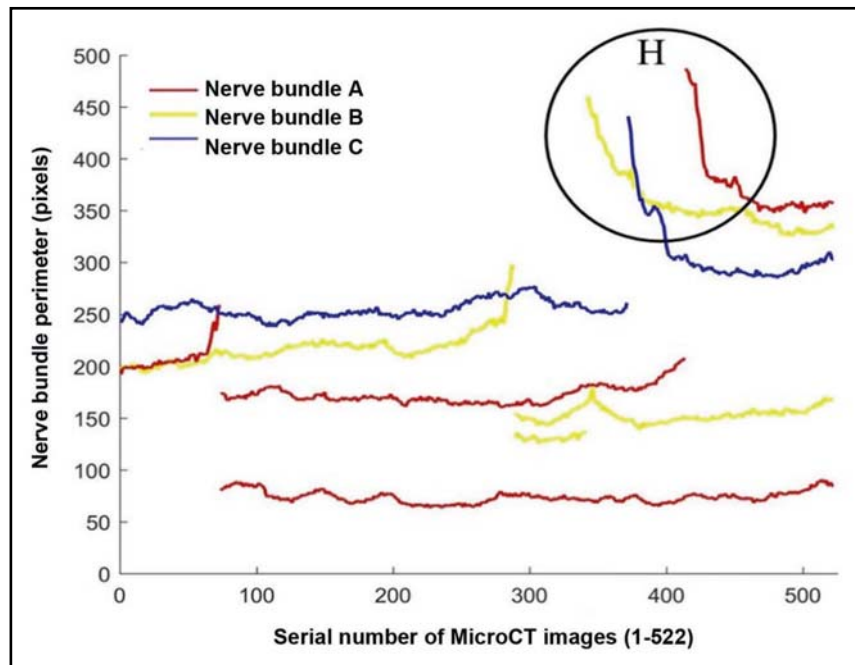


Fig. 6. Curve of perimeter variation of fascicular groups A, B and C during spatial extension.

probability density function curve of the fascicular group area, and the red curve denotes the cumulative probability density curve of *Beta* distribution, as illustrated in Figure 4:

- * The curve using *Beta* distribution extremely resembled the actual curve with a calculation error of 0.5%, meeting the requirement that the calculation error is less than 5%.
- * The cross-sectional area of the fascicular group followed *Beta* distribution. In general, the number of slender fascicular groups was the largest. The

thicker the fascicular group, the smaller the number of fascicular group.

Correlation between cross-sectional area and extension of fascicular group

To explicitly display the area changes of a single fascicular group in the process of spatial extension, three fascicular groups were randomly selected from the specimen, as illustrated in Figure 4. In the specimen shown in Figure 2A, the total number of scanning images is $m = 522$.

MicroCT images of three randomly selected fascicular groups A, B, C were illustrated in In Figure 4A. In Figure 4B, the red curve denotes the area change curve of the fascicular group A, the yellow curve for the fascicular group B, and the blue curve for the fascicular group C, respectively.

The discontinuity and fluctuation of the curve indicated that the splitting or merging occurred at this site, leading to sharp changes in the curve of the cross-sectional area of the fascicular group. During the spatial extension of a single fascicular group, the range of area change is not significant, of which 83.3% of the cross-sectional area of a single fascicular group fluctuated within a range of less than 1500 pixels. The cross-sectional area does not merely increase or decrease throughout the spatial extension of a single fascicular group, whereas it fluctuates at random regardless of the specific location.

Cross-sectional perimeter of single fascicular group

The statistical results of the cross-sectional perimeter of a single fascicular group were as follows without considering the perimeter of the fascicular group in the splitting and merging stages:



Fig. 7. The maximum degree of circularity of single fascicular group in the 338th image.

The maximum cross-sectional perimeter of a single fascicular group is $p_{max} = 455pixels$, which occurred in the fascicular group with the maximum area and the perimeter in Figure 2A.

The minimum cross-sectional perimeter of a single fascicular group is $p_{min} = 32pixels$, which was detected in the fascicular group with the minimum area and perimeter in Figure 2B.

The average cross-sectional perimeter of a single fascicular group is $p_{mean} = 202.8pixels$.

Histogram of the perimeter of fascicular group is illustrated in Figure 5A. According to the probability distribution fitting of the histogram, the cross-sectional perimeter of the fascicular group follows the normal distribution. The probability density function curve is expressed by the red curve, and the probability density function is:

$$f(x | \mu, \sigma) = \frac{1}{\sqrt{2\pi}\sigma} e^{-\frac{(x-\mu)^2}{2\sigma^2}} \quad (2)$$

In which, the mean $\mu = 202.8$ and $\sigma = 104.56$.

The histograms of the probability density and cumulative probability of fascicular group perimeter are illustrated in Figure 5A-B. The blue curve represents the actual cumulative probability density function curve and the red curve denotes the normally distributed cumulative probability density curve.

As illustrated in Figure 5B, the red curve was extremely close to the blue curve with an actual error of 0.8%, meeting the requirement that the error should be less than 5%. According to the statistical analysis of the fascicular group perimeter, the perimeter of a single fascicular group followed the normal distribution. The number of fascicular groups with a perimeter adjacent to the mean value was the largest, which significantly differed from the area distribution pattern

of a single fascicular group, suggesting that no interaction was observed between the area and perimeter of the fascicular group.

Correlation between perimeter and fascicular group extension

To clearly display the perimeter variation of a single fascicular group during the spatial extension, the results of three fascicular groups randomly selected from Figure 4A were illustrated in Figure 6.

In Figure 6, the perimeter changes of three fascicular groups in Figure 4A in the process of the spatial extension were represented in three different colors. The red curve denotes the perimeter change curve of fascicular group A, the yellow curve for fascicular group B, and the blue curve for fascicular group C.

The discontinuity and fluctuation of the perimeter curve of the fascicular groups indicated that splitting or merging occurred at this position, resulting in abrupt changes in the cross-sectional perimeter of the fascicular group. The variation range of the perimeter of a single fascicular group was relatively small in the process of spatial extension, of which 78.87% of the cross-sectional perimeter of a single fascicular group fluctuated for less than a range of 150 pixels. The perimeter of a single fascicular group fluctuated at random. The perimeter change curve of the fascicular group was illustrated in "H" position in Figure 6. The three curves within the "H" region were the obtained curves after the fascicular group merging or splitting, which presented with a rapid decline and then tended to stabilize. Similar situations could be obtained by analyzing the variation curves of the perimeter of other fascicular groups in the process of spatial extension. This phenomenon suggested that when the fascicular group was split or merged, the cross-sectional area of the fascicular group would stabilize immediately after the step change was completed, while the cross-sectional perimeter of the

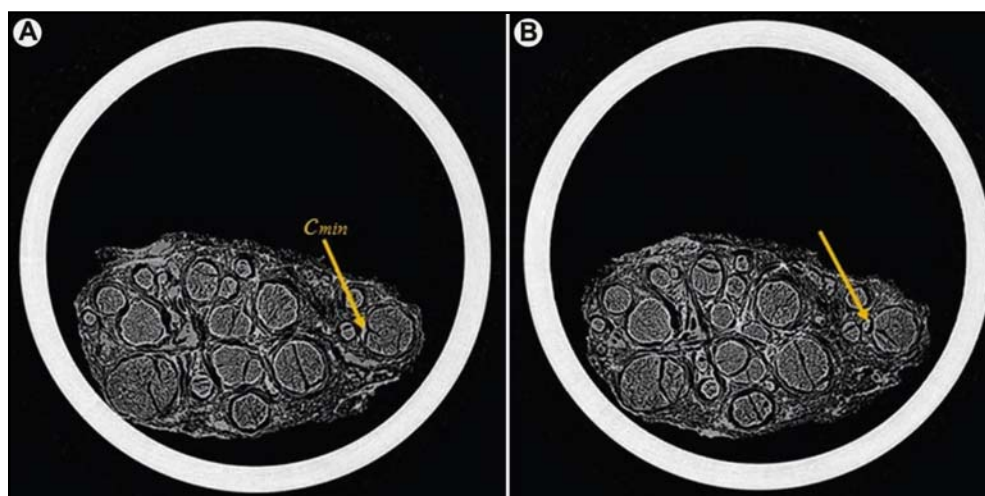


Fig. 8. Identification and development of the single fascicular group with the minimum degree of circularity. The minimum degree of circularity in the 260th scanning image (A); the new fascicular group developed into a normal fascicular group in the 310th scanning image.

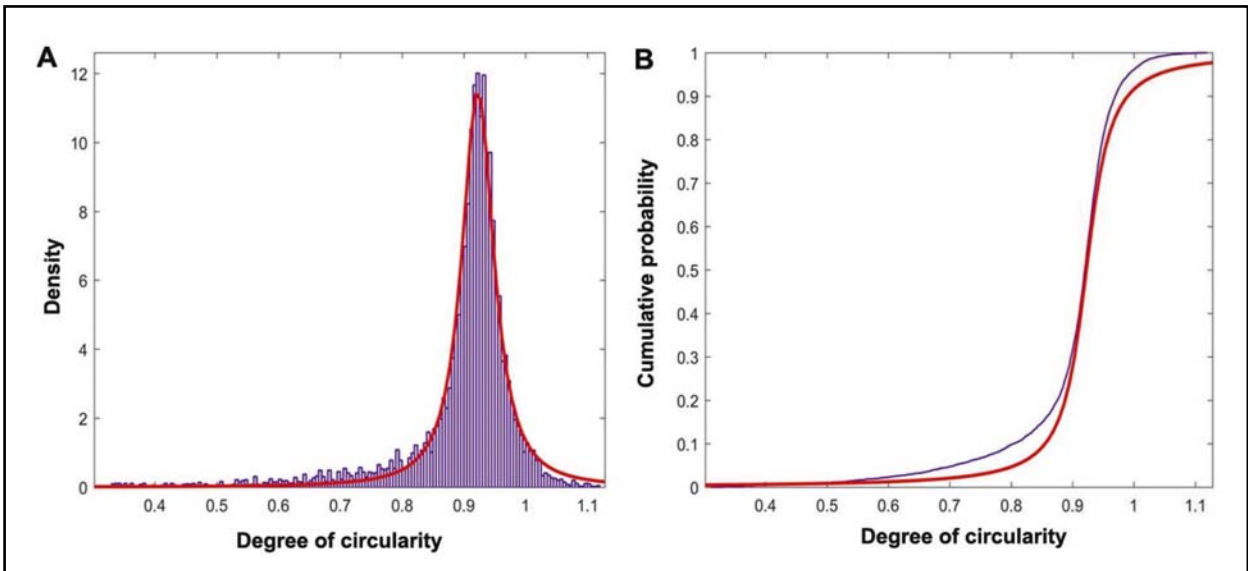


Fig. 9. The probability distribution of degree of circularity of fascicular groups; histogram of probability density of degree of circularity (A); cumulative probability of degree of circularity (B).

fascicular group would stabilize after a period of extension after the step change. After a step change, the cross-sectional perimeter of the fascicular group entered a stable extension stage with 25-35 scanning intervals. In this study, since the scanning interval between two images had been set to 5 μm when performing MicroCT scanning, the actual extension distance of the cross-sectional perimeter of the fascicular group after step change was calculated as (25~35)×5=(125~165) μm.

Cross-sectional degree of circularity of single fascicular group

Without considering the splitting and merging stages of the fascicular group, the statistical results of the cross-sectional degree of circularity of the single fascicular group were as follows: the maximum cross-sectional degree of circularity of the single fascicular group was: c_{max} -1.119, which occurred in the 338th image (Figure 7). According to the equation (6), the maximum degree of circularity can be obtained when the area is large and the perimeter is small.

The minimum cross-sectional degree of circularity of a single fascicular group was: c_{min} =0.3125 in the 260th image. As illustrated in Figure 8A, the fascicular group was slender and long in shape and split from the right fascicular group. It was difficult to perceive it as a fascicular group early after splitting. However, after an extension of approximately 50-unit scanning distance, the new fascicular group grew into a normal fascicular group in the 310th scanning image, as shown in Figure 8B. In this investigation, the scanning interval was set to 5 μm when acquiring the MicroCT scanning images. The new fascicular group completed the splitting process after a spatial extension for 50×5=250 μm. The mean degree of circularity of single fascicular group was c_{mean} =0.8987.

Histogram of the degree of circularity of fascicular groups was illustrated in Figure 9A. According to the probability distribution fitting of the histogram, the degree of circularity of fascicular groups followed the *t* distribution pattern with scale/position parameters, and the probability density function was as follows.

$$f_t(x) = \frac{\Gamma(\frac{\nu+1}{2})}{\sqrt{\nu\pi} \cdot \Gamma(\frac{\nu}{2})} (1 + \frac{x^2}{\nu})^{-\frac{\nu+1}{2}} \quad (7)$$

in which, Γ^* is gamma function, $\nu = 1.405$, $\sigma = 0.0293$ and $\mu = 0.923$.

The cumulative probability density curve of the degree of circularity of fascicular groups was shown in Figure 9. The blue curve refers to the actual cumulative probability density function curve of the cross-sectional degree of circularity of the fascicular group, and the red curve represents the cumulative probability density curve of the fitted *t* distribution with scale/position parameters. As illustrated in Figure 9B, the two curves were relatively similar. The actual error was 3.06%, meeting the requirement that the error was less than 5%.

Correlation analysis between cross-sectional degree of circularity and extension of single fascicular group

To explicitly display the changes of cross-sectional degree of circularity of a single fascicular group in the process of spatial extension, three fascicular groups in Figure 5A were taken as an example to show the results in Figure 10. The red curve refers to the degree of circularity change curve of fascicular group A, the yellow curve for fascicular group B, and the blue curve for fascicular group C.

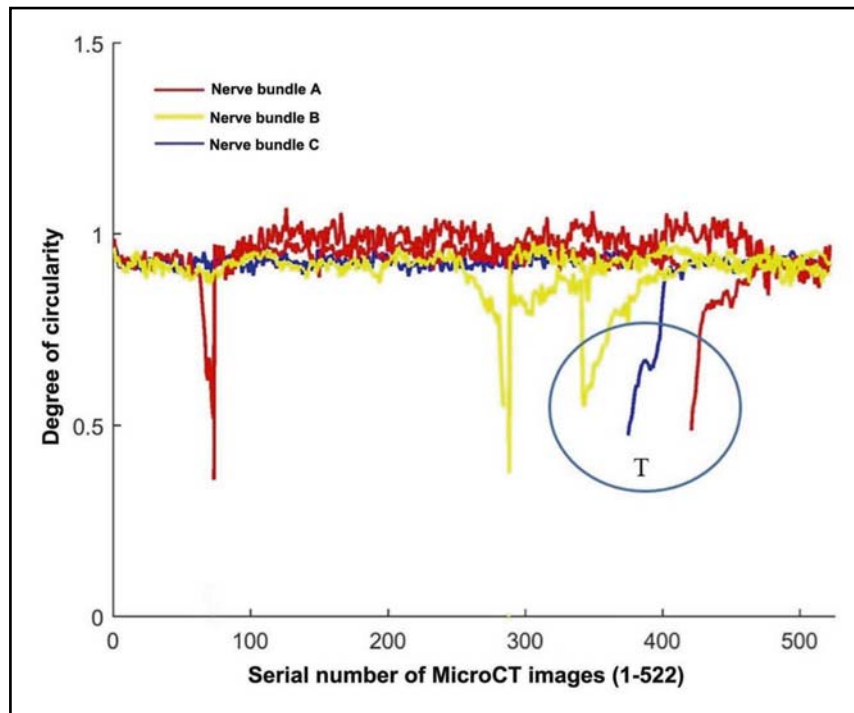


Fig. 10. Degree of circularity curves of fascicular groups A, B and C along the spatial extension of fascicular groups.

The discontinuity and fluctuation in the change curve of the degree of circularity of fascicular groups indicated that splitting or merging occurred at this position, resulting in sudden changes in the degree of circularity of fascicular groups. During the process of the spatial extension of a single fascicular group, the variation range of degree of circularity was extremely small, 97.2% of the cross-sectional degree of circularity of the fascicular groups fluctuated around the mean value. The degree of circularity fluctuated at random. The three curves within the “T” region in Figure 10 were the obtained curves after the fascicular group merging or splitting, which presented with a rapid increase and subsequently tended to stabilize. Considering the change curves of fascicular group area, perimeter, and degree of circularity, the fascicular group firstly presented with a long strip shape during splitting or merging, similar to the shape of the fascicular group marked “ c_{min} ” in Figure 8A, and then gradually resembled a circle shape.

DISCUSSION

Nerves are essential channels through which the human body can control limb movements and transmit limb sensory signals. Quantitative measurement and analysis of morphometric parameters of fascicular groups can provide an important basis for the clinical repair of nerves and diagnosis and treatment of neurological diseases.

In terms of quantitative measurement and analysis of morphometric parameters of nerve and interior

structures, Liu YC *et al.* have conducted quantitative measurement of nerve cells and myelin sheaths under a microscope (Liu *et al.* 2012). Li QL *et al.* have adopted molecular hyperspectral imaging technology to process the spinal nerves, obtain the microscopic images of nerve fibers, and extract morphometric parameters, such as myelin thickness and myelin area of nerve fibers (Liu *et al.* 2012). Scholars have quantitatively measured the morphometric parameters of a facial nerve adjacent to the fetal temporal bones. Irmina Jankowska-Lech *et al.* have measured the thickness of the peripapillary retinal nerve fiber layer (RNFL) (Jankowska-Lech 2019). In this study, the basic morphometric parameters of fascicular groups in the peripheral nerves, such as area, perimeter, and degree of circularity were quantitatively measured to obtain the overall probability distribution pattern of these parameters. By comparison, previous researches mainly focused on the microscopic level and had little association with the clinical diagnosis of peripheral nerve diseases. With the deepening research of this study, the diagnosis of peripheral nerve diseases can be determined by observing that whether the morphometric parameters of fascicular groups inside the peripheral nerves conform to statistical patterns. Therefore, the findings in the present investigation are of great clinical significance for the diagnosis of peripheral nerve diseases.

Regarding the correlation study of nerves, Shumoos Al-Fahdawi *et al.* have constructed the variation law of morphometric parameters, such as length, density, curvature, and thickness of optic nerve during the process of spatial extension, and also investigated the

error between these formulas and the actual situations (Al-Fahdawi *et al.* 2016). Talas *et al.* have explored the correlation between the length of the facial nerve and fetal weeks based on quantitative measurement of facial nerves (Talas *et al.* 2019). Irmina Jankowska-Lech *et al.* have established the correlation between peripapillary retinal nerve fiber layer (RNFL) thickness and neurodegenerative diseases (Jankowska-Lech 2019; Talas *et al.* 2019; Bikis *et al.* 2018a; Bikis *et al.* 2018b). In this article, according to the sequence of MicroCT scanning images, the values of cross-sectional area, perimeter, and degree of circularity of different fascicular groups were comprehensively measured and integrated to obtain the variation curves of basic cross-sectional morphometric parameters of fascicular groups along with the spatial extension of fascicular groups. Consequently, the correlation between the cross-sectional area, perimeter, and degree of circularity of fascicular groups and spatial extension could be obtained. The experimental results obtained from different specimens demonstrated that the cross-sectional area of the fascicular groups remained basically unchanged within the range of 3 mm, which was not significantly correlated with the extension of fascicular groups. However, the cross-sectional areas of the nerve and fascicular groups were smaller adjacent to the nerve end. It can be reasonably inferred that the cross-sectional area of the fascicular group does not gradually decrease during the spatial extension of the fascicular groups to the distal end, whereas it is likely that the cross-sectional area of the fascicular group suddenly decreases in a splitting manner. To our best knowledge, this is the first study to investigate this phenomenon, which has not been reported before.

In this investigation, the statistical pattern of the basic morphometric parameters of the fascicular groups inside the peripheral nerves was evaluated, and the variation pattern of these parameters of the fascicular groups in the process of the spatial extension was presented from the perspective of correlation analysis. Significantly different from previous studies, these findings in the present study are of great clinical significance for modifying the surgery of peripheral nerve injury. Due to limited experimental conditions, the sample size in this study is still relatively small. The results obtained from this study remain to be validated by subsequent investigations with large sample size.

In addition, the area, perimeter, and degree of circularity are the basic morphometric parameters for the quantitative description of fascicular groups. In this study, morphometric parameters, such as cross-sectional area, perimeter, degree of circularity of each fascicular group on each peripheral nerve MicroCT image were obtained through image processing and calculation, and then the maximum, average, and minimum values of these parameters of fascicular groups in the spatial extension process were statistically analyzed, and the correlation between these basic

morphometric parameters and the spatial extension of fascicular groups was evaluated. First, the cross-sectional area of fascicular groups obeys the *Beta* distribution pattern. Small area fascicular groups account for the dominant proportion. The cross-sectional area of fascicular groups is negatively associated with the number of fascicular groups. The larger the area of the fascicular group is, the smaller the number of fascicular groups is. Nevertheless, no significant correlation has been observed between the cross-sectional area and the spatial extension of the fascicular groups. Second, the cross-sectional perimeter of the fascicular groups follows the normal distribution pattern. The cross-sectional perimeter of the fascicular groups will not stabilize immediately after the fascicular group splits or merges, but tends to stabilize after extending for a certain distance. During this period, the cross-sectional perimeter of the fascicular group is gradually converging, and the cross-sectional area of the fascicular group has not been significantly changed, suggesting that after the fascicular group splitting or merging, the fascicular group tends to acquire a larger area and has higher capability against injury under the condition of occupying the same volume of tissue materials. Third, the cross-sectional degree of circularity of the fascicular group obeys the *t* distribution pattern with scale/position parameters. Corresponding to the cross-sectional perimeter of the fascicular group, the degree of circularity of the fascicular group tends to approach the average value merely after the fascicular group has split or merged. Fourth, in the process of the peripheral fascicular group extending to the extremity, the cross-sectional area of the fascicular group is not gradually reduced, and it is likely to suddenly decrease in a splitting manner.

In conclusion, to our best knowledge, this is the first study to quantitatively measure the basic morphometric parameters of fascicular groups within the peripheral nerves and obtain the statistical rules, reveal the general rules of the basic morphometric parameters of fascicular groups in the process of spatial extension, which provide a pivotal basis for the repair of peripheral nerves and the diagnosis and treatment of neurological diseases and are of academic value and significance.

CONCLUSION

In conclusion, this is the first study to quantitatively measure the basic morphometric parameters of fascicular groups within the peripheral nerves. The results uncovered the general rules associated with basic morphometric parameters of the fascicular groups in the process of spatial extension. The findings obtained from this study provide a pivotal basis for the repair of peripheral nerves. Therefore, these findings are not only of academic significance but also are valuable for the diagnosis and treatment of neurological diseases.

ACKNOWLEDGMENT

This study was supported by Natural Science Foundation Project of Guangdong Province, China (No. 2018A0303130137); Opening Project of Key Laboratory of High Performance Computation of Guangdong Province, China (No. TH1528); Science and Technology Project of Nanshan District, Shenzhen, China (No. 2018050); Science and Technology Project of Guangzhou of China (No. 201704030041) and Philosophy and Social Science Project of Guangdong Province, China (No. GD17XGL20).

CONFLICT OF INTEREST

The authors declare that they have no competing interests.

REFERENCES

- 1 Al-Fahdawi S, Qahwaji R, Al-Waisy AS, Ipson S, Malik RA, Brahma A, Chen X (2016). A fully automatic nerve segmentation and morphometric parameter quantification system for early diagnosis of diabetic neuropathy in corneal images. *Comput Methods Programs Biomed.* **135**: 151–166.
- 2 Bikis C, Degrugillier L, Thalmann P, Schulz G, Müller B, Hieber SE, Kalbermatten DF, Madduri S (2018). Three-dimensional imaging and analysis of entire peripheral nerves after repair and reconstruction. *J Neurosci Methods.* **295**: 37–44.
- 3 Bikis C, Thalmann P, Degrugillier L, Schulz G, Müller B, Kalbermatten DF, Madduri S, Hieber SE (2018). Three-dimensional and non-destructive characterization of nerves inside conduits using laboratory-based micro computed tomography. *J Neurosci Methods.* **294**: 59–66.
- 4 Felisaz PF, Poli A, Vitale R, Vitale G, Asteggiano C, Bergsland N, Callegari I, Vegezzi E, Piccolo L, Cortese A, Pichiecchio A, Bastianello S (2019). MR microneurography and quantitative T2 and DP measurements of the distal tibial nerve in CIDP. *J Neurol Sci.* **400**: 15–20.
- 5 Hopkins T.M., Heilman AM, Liggett JA, LaSance K, Little KJ, Hom DB, Minter DM, Marra KG, Pixley SK (2015). Combining micro-computed tomography with histology to analyze biomedical implants for peripheral nerve repair. *J Neurosci Methods.* **255**: 122–130.
- 6 Jankowska-Lech I, Wasyluk J, Palasik W, Terelak-Borys B, Grabka-Liberek I (2019). Peripapillary retinal nerve fiber layer thickness measured by optical coherence tomography in different clinical subtypes of multiple sclerosis. *Mult Scler Relat Disord.* **27**: 260–268.
- 7 John Hipp, et al (2009). The Neurovascular Supply of the Developing Vertebral Body: A MicroCT and Histologic Analysis of the Basivertebral Foramen, Nerve, and Vessels. *Spine J.* **9**: 146S.
- 8 Karlsson P, Haroutounian S, Polydefkis M, Nyengaard JR, Jensen TS (2016). Structural and functional characterization of nerve fibres in polyneuropathy and healthy subjects. *Scand J Pain.* **10**: 28–35.
- 9 Li Q, Chen Z, He X, Wang Y, Liu H, Xu Q (2012). Automatic identification and quantitative morphometry of unstained spinal nerve using molecular hyperspectral imaging technology. *Neurochem Int.* **61**: 1375–1384.
- 10 Liu YC. et al. (2012) Quantitative Measurement of Nerve Cells and Myelin Sheaths from Microscopic Images via Two-Stage Segmentation. In: Pan JS., Chen SM., Nguyen N.T. (eds) Intelligent Information and Database Systems. ACIDS 2012. Lecture Notes in Computer Science, vol 7198. Springer, Berlin, Heidelberg. https://doi.org/10.1007/978-3-642-28493-9_51.
- 11 Raj SD, Sweetwood K, Kapoor MM, Raj KM, Nagi C, Sepulveda KA, Sedgwick EL (2017). Spindle cell lesions of the breast: Multimodality imaging and clinical differentiation of pathologically similar neoplasms. *Eur J Radiol.* **90**: 60–72.
- 12 Rajjoub RD, Trimboli-Heidler C, Packer RJ, Avery RA (2015). Reproducibility of Retinal Nerve Fiber Layer Thickness Measures Using Eye Tracking in Children With Nonglaucomatous Optic Neuropathy. *Am J Ophthalmol.* **159**: 71–77. e1.
- 13 Talas DÜ, Beger O, Koç T, Hamzaoğlu V, Özalp H, Mavruk M, Yıldırım C, Güzelyüz İ, Vayisoğlu Y, Uzmansel D, Farsak M, Dağtekin A (2019). Morphometric properties of the facial nerve in fetal temporal bones. *Int J Pediatr Otorhinolaryngol.* **116**: 7–14.
- 14 Watling C.P., Lago N, Benmerah S, FitzGerald JJ, Tarte E, McMahon S, Lacour SP, Cameron RE (2010). Novel use of X-ray micro computed tomography to image rat sciatic nerve and integration into scaffold. *J Neurosci Methods.* **188**: 39–44.
- 15 Yan L, Guo Y, Qi J, Zhu Q, Gu L, Zheng C, Lin T, Lu Y, Zeng Z, Yu S, Zhu S, Zhou X, Zhang X, Du Y, Yao Z, Lu Y, Liu X (2017). Iodine and freeze-drying enhanced high-resolution MicroCT imaging for reconstructing 3D intraneural topography of human peripheral nerve fascicles. *J Neurosci Methods.* **287**: 58–67.
- 16 Zhang Y, Qi J, Liu X, X Z, Li S (2009). Three-dimensional reconstruction of functional fascicular groups inside a segment of common peroneal nerve. *J Bioact Compat Pol.* **24**: 100–112.
- 17 Zhong Y, Zhang M, Qi J, Liu X (2011). Study on Discrete Nerve Fascicular Groups Edge Extraction from Slice Image. *J System Simulation.* **11**: 1414–1418.
- 18 Zhong Y, Luo P (2012). Type recognition of fascicular groups from nerve slice image. *J Image and Graphics.* **17**: 82–89.
- 19 Zhong Y, Wang L, Dong J, Zhang Y, Luo P, Qi J, Liu X, Xian CJ (2015). Three-dimensional Reconstruction of Peripheral Nerve Internal Fascicular Groups. *Sci Rep.* **5**: 17168.
- 20 Zhu S, Zhu Q, Liu X, Yang W, Jian Y, Zhou X, He B, Gu L, Yan L, Lin T, Xiang J, Qi J (2016). Three-dimensional Reconstruction of the Microstructure of Human Acellular Nerve Allograft. *Sci Rep.* **6**: 30694.